AJNR

Quantitative Assessment of Circumferential Enhancement along the Wall of Cerebral Aneurysms Using MR Imaging

S. Omodaka, H. Endo, K. Niizuma, M. Fujimura, T. Inoue, K. Sato, S.-i. Sugiyama and T. Tominaga

Quantitative Assessment of Circumferential Enhancement along the Wall of Cerebral Aneurysms Using MR Imaging

S. Omodaka, H. Endo, K. Niizuma, M. Fujimura, T. Inoue, K. Sato, S.-i. Sugiyama, and T. Tominaga

ABSTRACT

BACKGROUND AND PURPOSE: The incidence of wall enhancement of cerebral aneurysms on vessel wall MR imaging has been described as higher in ruptured intracranial aneurysms than in unruptured intracranial aneurysms, but the difference in the degree of enhancement between ruptured and unruptured aneurysms is unknown. We compared the degree of enhancement between ruptured and unruptured intracranial aneurysms by using quantitative MR imaging measures.

MATERIALS AND METHODS: We performed quantitative analyses of circumferential enhancement along the wall of cerebral aneurysms in 28 ruptured and 76 unruptured consecutive cases by using vessel wall MR imaging. A 3D-T1-weighted fast spin-echo sequence was obtained before and after contrast media injection, and the wall enhancement index was calculated. We then compared characteristics between ruptured and unruptured aneurysms.

RESULTS: The wall enhancement index was significantly higher in ruptured than in unruptured aneurysms (1.70 ± 1.06 versus 0.89 ± 0.88, respectively; $P = .0001$). The receiver operating characteristic curve analysis found that the most reliable cutoff value of the wall enhancement index to differentiate ruptured from unruptured aneurysms was 0.53 (sensitivity, 0.96; specificity, 0.47). The wall enhancement index remained significant in the multivariate logistic regression analysis ($P < .0001$).

CONCLUSIONS: Greater circumferential enhancement along the wall of cerebral aneurysms correlates with the ruptured state. A quantitative evaluation of circumferential enhancement by using vessel wall MR imaging could be useful in differentiating ruptured from unruptured intracranial aneurysms.

ABBREVIATIONS: CR = contrast ratio; SI = signal intensity; WEI = wall enhancement index

Vessel wall MR imaging with a 3D-T1-weighted FSE sequence has been increasingly used to study intracranial vascular lesions such as atherosclerosis, vasculitis, and aneurysms.[1-4] Previous reports established a link between ruptured aneurysms and wall enhancement by using qualitative vessel wall MR imaging assessments.[1,5,6] However wall enhancement was also observed in unruptured aneurysms[1,6]; thus, we hypothesized that the degree of enhancement is higher in ruptured than in unruptured aneurysms. In this study, we used a quantitative method to compare the degree of enhancement between ruptured and unruptured intracranial aneurysms by using a 3D-T1WI FSE sequence.

MATERIALS AND METHODS

Study Population and Data Extraction

This study was approved by an institutional review board (Kohnan Hospital). Patient data were extracted from an institutional data base, which includes consecutive patients with surgically treated intracranial aneurysms. We included all patients with intracranial aneurysms surgically treated between December 2013 and May 2015. The exclusion criteria were the following: 1) the absence of preoperative MR imaging or 3D angiography data, 2) an aneurysm of <2 mm or >12 mm, 3) a previously treated aneurysm, 4) insufficient MR imaging quality to evaluate circumferential enhancement along the wall of the aneurysm, 5) a fusiform or partially thrombosed aneurysm, and 6) an unruptured aneurysm complicated by a ruptured aneurysm.

Imaging Protocol

A 3T or 1.5T MR imaging scanner (Signa HDxt; GE Healthcare, Milwaukee, Wisconsin) was used in this study. The vessel wall MR
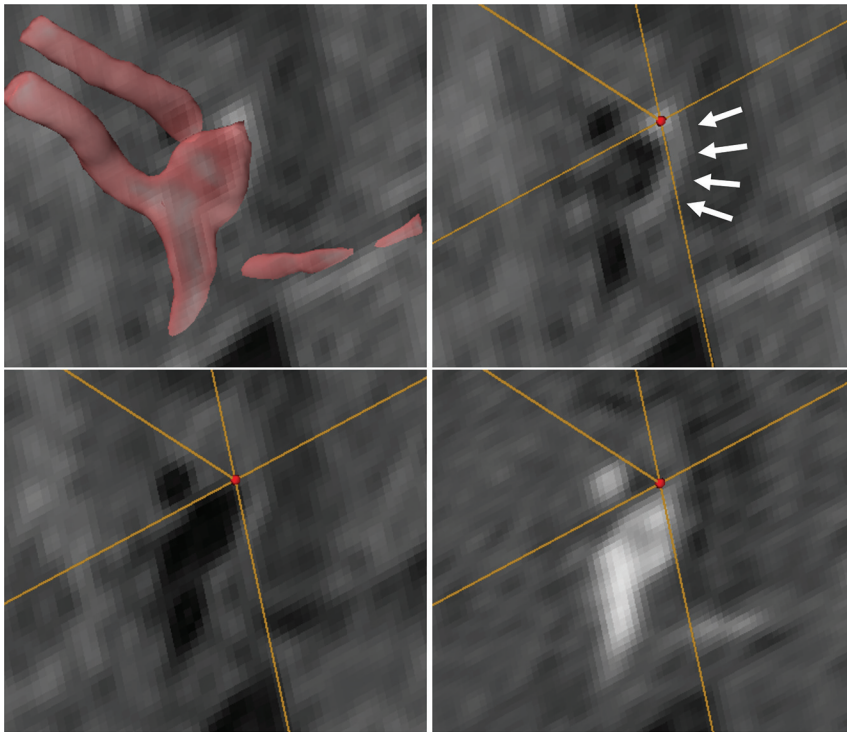
FIG 1. Images from a 40-year-old man with a ruptured anterior communicating artery aneurysm. Transparent volume-rendering of a 3D-TOF imaging is superimposed on an axial section of post-contrast TIWI (*upper left*). A VOI (*red dot*) is set on the enhanced aneurysmal wall on matched post- (*upper right*) and precontrast TIWI (*lower left*) and TOF (*lower right*) image. *Arrows* indicate the circumferential enhancement along the wall of the ruptured aneurysm (*upper right*).

terize the extent of the enhancement. We defined the VOI with the highest signal intensity (SI) as follows: First, we set a cubic VOI (volume of 0.125 mm^3) on a visible enhanced region along the aneurysm wall on the 3D-T1WI FSE sequence while we checked the aneurysm configuration referencing the volume-rendering of 3D-TOF imaging. Next, we manually traced the enhanced region by moving the VOI, avoiding surrounding structures, while we checked the SI of the VOI, which was automatically calculated and displayed in real-time. We recorded several values of VOI with high average SI and finally defined the highest average SI from these candidate values. The highest SI within the VOI on the matched pre- and postcontrast images was measured (SI$_{wall}$, Figs 1–3). The SI of normal brain parenchyma (SI$_{brain}$) averaged in a volume of 8.0 mm^3 on matched pre- and postcontrast imaging was measured in the right frontal lobe as a reference. The SI of the stalk (SI$_{stalk}$) averaged in a volume of 1.0 mm^3 on matched pre- and postcontrast images was also measured. Then, the WEI was calculated as follows: ([SI$_{wall}$/SI$_{brain}$ on postcontrast imaging] − [SI$_{wall}$/SI$_{brain}$ on matched precontrast imaging])/(SI$_{wall}$/SI$_{brain}$ on matched precontrast imaging). The stalk enhancement index was calculated in a similar way. The contrast ratio of the circumference of the aneurysm against the stalk (CR$_{stalk}$) was calculated as follows: SI$_{wall}$/SI$_{stalk}$ on postcontrast imaging. In the initial 20 patients, the SI$_{wall}$, SI$_{brain}$, and SI$_{stalk}$ on matched pre- and postcontrast imaging were measured by the reviewer again and then by a different reviewer who was also blinded to the clinical data but aware of the aneurysm location for an estimation of intra- and interobserver variability.

imaging consisted of the single-slab 3D-T1WI FSE pulse sequence.[7] We also performed 3D-TOF MR imaging. The acquisition parameters are summarized in On-line Tables 1 and 2. Gadodiamide (Omniscan; GE Healthcare, Piscataway, New Jersey) or gadopentetate dimeglumine (Magnevist; Bayer HealthCare Pharmaceuticals, Wayne, New Jersey) was administered intravenously (0.1 mmol/kg), and the 3D-T1WI FSE sequence was repeated 5 minutes after the contrast material was administered. The voxel data were exported into a personal computer for intensity analysis.

3D rotational angiography was performed by using an Innova 3131 IQ or IGS 630 scanner (GE Healthcare). Rotational angiographic images were obtained during a 200° rotation with imaging at 30 frames/s for 5 seconds The corresponding 150 projection images were reconstructed into a 3D dataset of 512 × 512 × 512 voxels covering an FOV of 116 mm on a dedicated GE Healthcare Z800 workstation. The aneurysm location was classified as the anterior cerebral arteries, the posterior communicating artery, an internal carotid artery other than posterior communicating artery, a middle cerebral artery, and the posterior circulation, as described previously.[8] The maximum measurement of aneurysm diameter was used as the aneurysm size.

Measurement of the Aneurysmal Wall Enhancement
Multiplanar oblique reconstructions obtained from pre- and postcontrast 3D-T1WI FSE and 3D-TOF were analyzed after coregistration with Amira 5.3 (www.amira.com). The reviewer was blinded to the clinical data but was aware of the aneurysm location. The circumferential enhancement along the wall of the aneurysm (wall enhancement index [WEI]) was used to charac-

Data Analysis
Continuous variables are presented as the mean ± SD, and categoric variables are presented as a number and corresponding percentage. The characteristics of ruptured and unruptured aneurysms were compared with the Student *t* test for continuous variables and the χ^2 or Fisher exact test for categoric variables. A 2-sided *P* value < .05 was considered significant. The cutoff values of variables with the best sensitivity and specificity for differentiating ruptured from unruptured aneurysms were identified by analyzing the receiver operating characteristic curve, and they were used in further analysis. Multivariate logistic regression analysis was performed to determine factors independently associated with ruptured aneurysms, including variables that reached *P* values < .2 in the univariate analysis. To determine the intra- and interobserver variability, we used the intraclass correlation coefficient with a 95% CI to assess the intra- and interobserver variability of the WEI and CR$_{stalk}$ calculations. All statistical analyses were performed
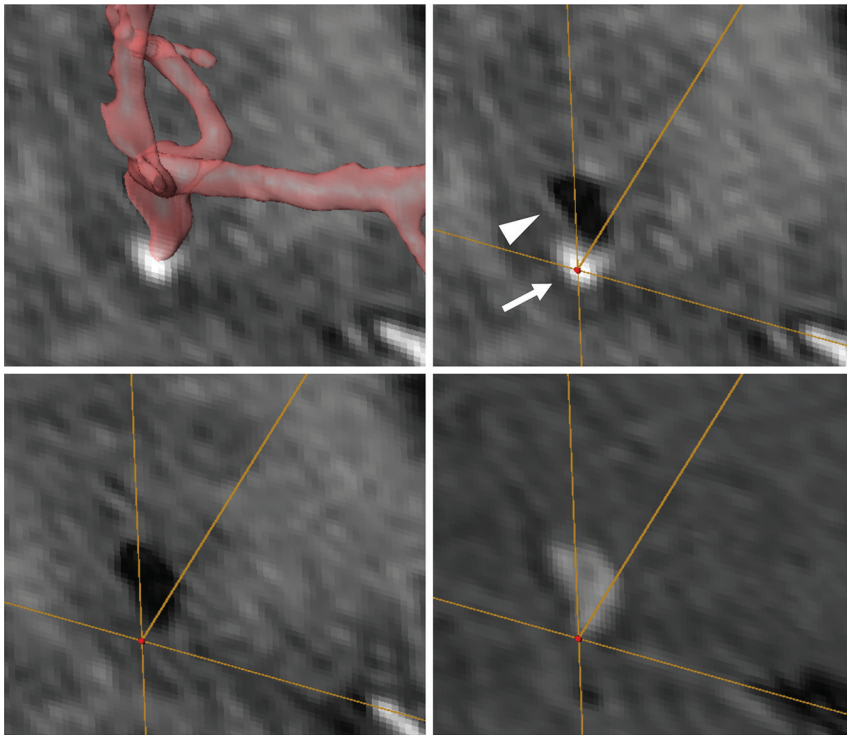
FIG 2. Images from a 52-year-old man with a ruptured left middle cerebral artery aneurysm. Transparent volume-rendering of a 3D-TOF imaging is superimposed on a coronal section of postcontrast TIWI (*upper left*). A VOI (*red dot*) is set on the enhanced aneurysmal wall on matched post- (*upper right*) and precontrast TIWI (*lower left*) and TOF (*lower right*) image. Circumferential enhancement along the wall of the aneurysm (*arrowhead*) was heterogeneous and locally enhanced (*arrow*) around the bleb in this case (*upper right*).
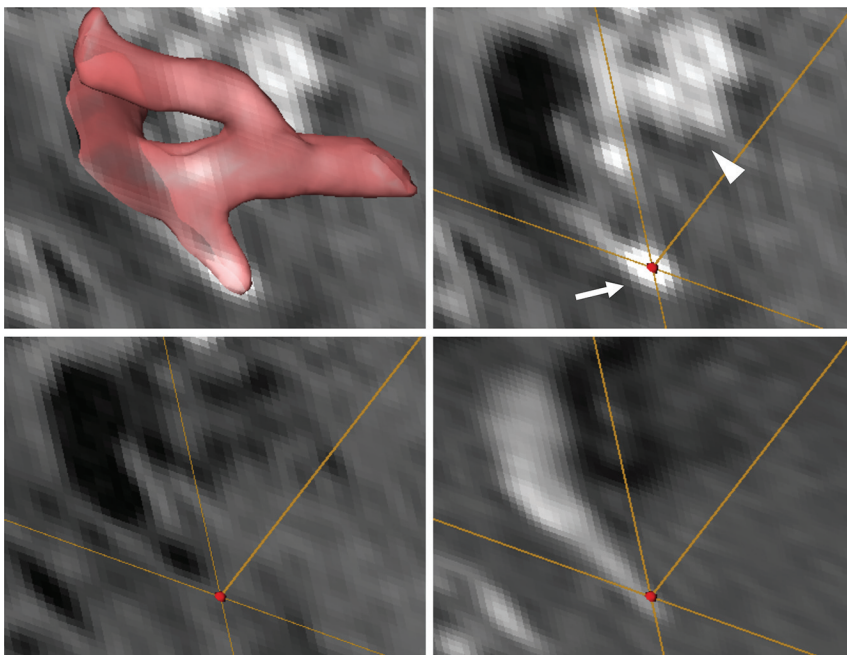
FIG 3. Images from a 55-year-old woman with a ruptured right anterior choroidal artery aneurysm. Transparent volume-rendering of a 3D-TOF imaging is superimposed on an axial section of postcontrast TIWI (*upper left*). A VOI (*red dot*) is set on the enhanced aneurysmal wall on matched post- (*upper right*) and precontrast TIWI (*lower left*) and TOF (*lower right*) image. In addition to the circumferential enhancement along the wall of the aneurysm (*arrow, upper right*), the cavernous sinus surrounding the proximal internal carotid artery was also enhanced (*arrowhead, upper right*); enhancement of the cavernous sinus is one of the confounding factors in the interpretation of circumferential enhancement along the wall of the aneurysm.

with JMP Pro 10.2 (SAS Institute, Cary, North Carolina) or SPSS Statistics 19.0 (IBM, Armonk, New York).

RESULTS

Of the 171 included patients, 89 were excluded because of the absence of MR imaging or 3D angiographic data ($n = 62$), for having an aneurysm size <2 mm or >12 mm ($n = 12$), for having a previously treated aneurysm ($n = 7$), for insufficient MR imaging quality ($n = 4$), or for the presence of a fusiform aneurysm ($n = 4$). The final study sample included 82 patients with 104 aneurysms (28 ruptured and 76 unruptured). In the ruptured aneurysms, MR imaging was performed on day 0 or 1 from the onset of the rupture in 24 (85.7%), on day 3 or 4 in 3 (10.7%), and on day 13 in 1 (3.6%) patient. All unruptured aneurysms were asymptomatic.

The results of the univariate analysis are summarized in Table 1. The WEI was significantly higher in ruptured than in unruptured aneurysms (1.70 ± 1.06 versus 0.89 ± 0.88, respectively; $P = .0001$). Among the other clinical variables, age and CR_{stalk} were significantly related to having a ruptured aneurysm. The receiver operating characteristic curves (Fig 4) indicated that the most reliable cutoff values of the WEI and CR_{stalk} to differentiate ruptured and unruptured aneurysms were 0.53 and 0.64, respectively (the areas under the curve were 0.75 and 0.84, respectively). When the cutoff value of the WEI was 0.53, the sensitivity and specificity were 0.96 and 0.47, respectively. When the cutoff value of the CR_{stalk} was 0.64, the sensitivity and specificity were 0.75 and 0.83, respectively. The results of the multivariate analysis are summarized in Table 2. The WEI remained significant in the multivariate analysis (OR, 22.91; 95% CI, 4.59–142.08; $P < .0001$). The intraobserver variability was excellent for the WEI (intraclass correlation coefficient, 0.94; 95% CI, 0.86–0.98) and CR_{stalk} (intraclass correlation coefficient, 0.98; 95% CI, 0.94–0.99). The interobserver variability was also excellent for the WEI (intraclass correlation coefficient, 0.92; 95% CI, 0.81–0.97) and CR_{stalk} (intraclass correlation coefficient, 0.98; 95% CI, 0.95–0.99).

Table 1: Characteristics of ruptured and unruptured intracranial aneurysms[a]

Characteristics	Ruptured (n = 28)	Unruptured (n = 76)	P Value
Age (yr)	58.5 ± 11.6	63.8 ± 9.4	.019
Women (No.) (%)	20 (71.4)	60 (79.0)	.439
Aneurysm location (No.) (%)			.087
Anterior cerebral arteries	6 (21.4)	12 (15.8)	
Posterior communicating artery	7 (25.0)	9 (11.8)	
Internal carotid artery other than posterior communicating artery	3 (10.7)	12 (15.8)	
Middle cerebral artery	9 (32.1)	41 (54.0)	
Posterior circulation	3 (10.7)	2 (2.6)	
Aneurysm size (mm)	5.4 ± 2.2	5.4 ± 2.1	.932
MR imaging quantitative measures			
Wall enhancement index	1.70 ± 1.06	0.89 ± 0.88	.0001
Stalk enhancement index	1.61 ± 0.42	1.71 ± 0.36	.214
Contrast ratio against the stalk	0.88 ± 0.40	0.45 ± 0.23	<.0001

[a] The data of continuous variables are mean ± SD.
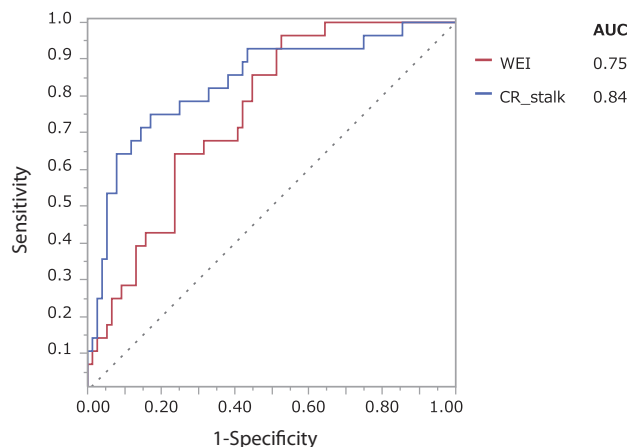
FIG 4. Receiver operating characteristic curves of the wall enhancement index (red) and the contrast ratio against the stalk (blue) in differentiating ruptured from unruptured aneurysms. The areas under the curve for the WEI and CR$_{stalk}$ are 0.75 and 0.84, respectively.

Table 2: Multivariate logistic regression analysis for factors associated with ruptured aneurysms

	P Value	OR (95% CI)
Age < cutoff	.0042	4.94 (1.62–17.85)
Aneurysm location[a]	.0014	6.77 (1.92–19.90)
Wall enhancement index > cutoff	<.0001	22.91 (4.59–142.08)

[a] Including anterior cerebral arteries, the internal carotid artery other than the posterior communicating artery, and the posterior circulation.

DISCUSSION

Our study used quantitative measures to demonstrate that the degree of circumferential enhancement along the wall of a cerebral aneurysm is significantly higher in ruptured than unruptured aneurysms. To our knowledge, this is the first report that quantitatively analyzes the degree of wall enhancement of cerebral aneurysms by using MR imaging.

Recently, wall enhancement of a cerebral aneurysm has been revealed as a characteristic of ruptured aneurysms by using vessel wall MR imaging. Matouk et al[5] investigated 5 patients with aneurysmal subarachnoid hemorrhage, including 3 patients with multiple aneurysms. All ruptured aneurysms had wall enhancement, and none of the associated unruptured aneurysms demonstrated this trait. Nagahata et al[6] investigated the frequency of wall enhancement in 61 ruptured and 83 unruptured aneurysms by using a 3D-T1WI turbo spin-echo sequence. They classified the wall enhancement into 3 groups: strong, faint, and no enhancement. Strong enhancement of the aneurysm wall, which was defined as equal to that of the choroid plexus or venous plexus, was observed in 73.8% of ruptured aneurysms and in 4.8% of unruptured aneurysms. They found a higher degree of enhancement in ruptured aneurysms compared with unruptured aneurysms. Edjlali et al[1] investigated wall enhancement in 108 aneurysms by using a 3D-T1WI FSE sequence and found that wall enhancement was significantly more frequently observed in unstable (ruptured, symptomatic, or undergoing morphologic modification) than stable (incidental and nonevolving) intracranial aneurysms (87% versus 28.5%, respectively). These reports used qualitative assessments to demonstrate that the wall is frequently enhanced in ruptured aneurysms and infrequently enhanced in unruptured aneurysms.

In the present study, we show that the degree of circumferential enhancement along the wall of the aneurysm is significantly higher in ruptured than unruptured aneurysms by using a 3D-T1WI FSE sequence. In unruptured aneurysms, atherosclerosis, inflammation, and the development of vasa vasorum were thought to be possible mechanisms of this enhancement effect.[1,9] In ruptured aneurysms, physical disruption and endothelial damage or an inflammatory healing process could explain this enhancement effect.[5,10] Our results indicated that such mechanisms of enhancement in ruptured aneurysms could be associated with a higher degree of enhancement compared with unruptured aneurysms. Wall enhancement may be an indicator of a ruptured aneurysm, which is useful information for managing patients with subarachnoid hemorrhage, especially those with multiple aneurysms or microaneurysms.[4,5] In ruptured aneurysms, this enhancement would correspond not to the wall enhancement itself but to enhancement of the interface between aneurysm wall and the surrounding brain tissue. The bleb of the aneurysm, which was likely to be the ruptured site, was locally enhanced in some cases (Fig 2). Thrombus or the platelet plug within or around the ruptured site might be enhanced in these cases. Visualization of the aneurysm wall itself has been attempted by using various magnetic fields from 1.5T to 7T.[11-13] In these studies, the aneurysm wall thickness showed spatial variation within the aneurysm compared with the wall of the parent artery. The intensity of the wall is equal to the intensity of brain tissue; therefore, it is difficult to achieve complete visualization of the entire wall of the cerebral aneurysm, even by high-resolution MR imaging.[12] These studies would indicate the difficulty of visualizing the aneurysm wall itself. Thus, we describe the enhancement effect of cerebral aneurysms as "circumferential enhancement along the wall." Further study is needed to prove the exact mechanisms of this enhancement effect.

The quantitative assessment of wall enhancement has been reported for intracranial atherosclerotic lesions by using vessel wall MR imaging.[14,15] Similarly, we calculated the WEI and applied it to the quantitative assessment of the enhancement effect. Our re-

sults demonstrate that the quantitative assessment of circumferential enhancement along the wall by using a 3D-T1WI FSE sequence could be useful in diagnosing the ruptured aneurysmal state, and the most reliable cutoff value of the WEI for the differentiation of ruptured and unruptured aneurysms was 0.53. Because the SI on MR imaging varies considerably with different parameter settings, this cutoff value itself cannot be generalized. However, this study certainly shows that higher WEIs are closely related to a ruptured state.

Furthermore, the CR_{stalk} was also significantly higher in ruptured than in unruptured aneurysms. The CR_{stalk} was also a reliable measure for the differentiation of ruptured and unruptured aneurysms in the receiver operating characteristic analysis. CR_{stalk} can be obtained only from the postcontrast imaging, while both pre- and postcontrast MR imaging is necessary to calculate WEI. CR_{stalk} can reduce imaging time and would be convenient to use in daily practice. However, attention should be paid to the interpretation of circumferential enhancement along the wall of the aneurysm because of the presence of confounding factors. Vasculature with low blood flow velocity, such as aneurysms with intra-aneurysmal flow stagnation and surrounding veins, could be enhanced and potentially confusing. We excluded aneurysms of >12 mm because this intra-aneurysmal flow stagnation effect would occur in larger aneurysms. In addition, structures adjacent to the aneurysms with strong enhancements, such as the dura and venous sinus, or with high intensity on T1-weighted imaging, such as skull and hematomas, may obscure subtle wall enhancement (Fig 3). Thus, it would be difficult to assess the WEI of paraclinoid aneurysms, which are located adjacent to the cavernous sinus and skull base dura. Both pre- and postcontrast imaging should be compared to accurately assess wall enhancement of cerebral aneurysms in these confusing situations.

In addition to the above-mentioned tips for the interpretation of a 3D-T1WI FSE sequence, our study has several limitations. First, the sample size was small because this was a single-center study. Second, the findings obtained by MR imaging are without histologic verification because of the difficulty of obtaining specimens from aneurysms. Third, this study focused only on surgically treated patients. This selection bias could explain why the patients with unruptured aneurysms were significantly older and why many more aneurysms were located in the middle cerebral artery. Fourth, we analyzed the data obtained at both 1.5T and 3 T. The signal-to-noise ratio and spatial resolution at 1.5T appeared to be somewhat insufficient for the precise evaluation of minute intramural lesions in the intracranial artery, which was the reason we excluded small aneurysms of <2 mm. The aneurysm wall and its variation in thickness can be more clearly visualized with higher magnetic fields.[12] Finally, we could not assess the causal relationship between circumferential enhancement and aneurysm rupture because of the retrospective design of this study. A prospective study with a larger number of patients using high-resolution MR imaging would provide more evidence for the association we indicated in the present study.

CONCLUSIONS

Our study quantitatively compared the degree of circumferential enhancement along the wall of ruptured and unruptured cerebral aneurysms by using a 3D-T1WI FSE sequence. Patients with greater enhancement are more likely to have ruptured aneurysms, which is useful information for managing patients with subarachnoid hemorrhage.

REFERENCES

1. Edjlali M, Gentric JC, Régent-Rodriguez C, et al. **Does aneurysmal wall enhancement on vessel wall MRI help to distinguish stable from unstable intracranial aneurysms?** *Stroke* 2014;45:3704–06 CrossRef Medline

2. Natori T, Sasaki M, Miyoshi M, et al. **Evaluating middle cerebral artery atherosclerotic lesions in acute ischemic stroke using magnetic resonance T1-weighted 3-dimensional vessel wall imaging.** *J Stroke Cerebrovasc Dis* 2014;23:706–11 CrossRef Medline

3. Dieleman N, van der Kolk AG, Zwanenburg JJ, et al. **Imaging intracranial vessel wall pathology with magnetic resonance imaging: current prospects and future directions.** *Circulation* 2014;130:192–201 CrossRef Medline

4. Endo H, Niizuma K, Fujimura M, et al. **Ruptured cerebral microaneurysm diagnosed by 3-dimensional fast spin-echo T1 imaging with variable flip angles.** *J Stroke Cerebrovasc Dis* 2015;24:e231–35 CrossRef Medline

5. Matouk CC, Mandell DM, Günel M, et al. **Vessel wall magnetic resonance imaging identifies the site of rupture in patients with multiple intracranial aneurysms: proof of principle.** *Neurosurgery* 2013; 72:492–96; discussion 496 CrossRef Medline

6. Nagahata S, Nagahata M, Obara M, et al. **Wall enhancement of the intracranial aneurysms revealed by magnetic resonance vessel wall imaging using three-dimensional turbo spin-echo sequence with motion-sensitized driven-equilibrium: a sign of ruptured aneurysm?** *Clin Neuroradiol* 2014 Oct 21. [Epub ahead of print] Medline

7. Mugler JP 3rd. **Optimized three-dimensional fast-spin-echo MRI.** *J Magn Reson Imaging* 2014;39:745–67 CrossRef Medline

8. Greving JP, Wermer MJ, Brown RD Jr, et al. **Development of the PHASES score for prediction of risk of rupture of intracranial aneurysms: a pooled analysis of six prospective cohort studies.** *Lancet Neurol* 2014;13:59–66 CrossRef Medline

9. Portanova A, Hakakian N, Mikulis DJ, et al. **Intracranial vasa vasorum: insights and implications for imaging.** *Radiology* 2013; 267:667–79 CrossRef Medline

10. Krings T, Mandell DM, Kiehl TR, et al. **Intracranial aneurysms: from vessel wall pathology to therapeutic approach.** *Nat Rev Neurol* 2011; 7:547–59 CrossRef Medline

11. Matsushige T, Akiyama Y, Okazaki T, et al. **Vascular wall imaging of unruptured cerebral aneurysms with a hybrid of opposite-contrast MR angiography.** *AJNR Am J Neuroradiol* 2015;36:1507–11 CrossRef Medline

12. Kleinloog R, Korkmaz E, Zwanenburg JJ, et al. **Visualization of the aneurysm wall: a 7.0-Tesla magnetic resonance imaging study.** *Neurosurgery* 2014;75:614–22; discussion 622 CrossRef Medline

13. Park JK, Lee CS, Sim KB, et al. **Imaging of the walls of saccular cerebral aneurysms with double inversion recovery black-blood sequence.** *J Magn Reson Imaging* 2009;30:1179–83 CrossRef Medline

14. Qiao Y, Zeiler SR, Mirbagheri S, et al. **Intracranial plaque enhancement in patients with cerebrovascular events on high-spatial-resolution MR images.** *Radiology* 2014;271:534–42 CrossRef Medline

15. Lou X, Ma N, Ma L, et al. **Contrast-enhanced 3T high-resolution MR imaging in symptomatic atherosclerotic basilar artery stenosis.** *AJNR Am J Neuroradiol* 2013;34:513–17 CrossRef Medline